International Journal of Thermal Sciences 49 (2010) 534–542

Contents lists available at ScienceDirect

International Journal of Thermal Sciences

journal homepage: www.elsevier.com/locate/ijts

The effect of Lewis and Damköhler numbers on the flame propagation through micro-organic dust particles

Mehdi Bidabadi*, Ali Haghiri, Alireza Rahbari

Department of Mechanical Engineering, Iran University of Science and Technology (IUST), Combustion Research Laboratory, Tehran, Iran

ARTICLE INFO

Article history:
Received 28 December 2008
Received in revised form
27 August 2009
Accepted 5 October 2009
Available online 21 October 2009

Keywords:
Dust particles
Lewis number
Damköhler number
Gaseous fuel mass fraction
Organic dust mass fraction
Burning velocity
Asymptotic analysis

ABSTRACT

In this study, the role of Lewis and Damköhler numbers on the premixed flame propagation through micro-organic dust particles is investigated. It is presumed that the fuel particles vaporize first to yield a gaseous fuel, which is oxidized in the gas phase. In order to simulate the combustion process, the flame structure is composed of four zones; a preheat zone, a vaporization zone, a reaction zone and finally a post flame zone, respectively. Then the governing equations, required boundary conditions and matching conditions are applied for each zone and the standard asymptotic method is used in order to solve these differential equations. Consequently the important parameters on the combustion phenomenon of organic dust particles such as gaseous fuel mass fraction, organic dust mass fraction and burning velocity with the various numbers of Lewis, Damköhler and the onset of vaporization are plotted in figures. This prediction has a reasonable agreement with experimental data of micro-organic dust particle combustion.

1. Introduction

Dust explosions are the phenomena that flame propagates through dust clouds in air with increasing degree of subdivision of any combustible solids. They have been a recognized threat to humans and property for the last 150 years [1]. In industries that manufacture, process, generate, or use combustible dusts, an accurate knowledge of their explosion hazards is essential [2]. With the advancement of powder technology and the increase of powder handling processes, hazard assessment and the establishment of preventive methods for dust explosions have become more important from the viewpoint of industrial loss prevention [1].

In spite of significant efforts to obtain information on the explosibility of dusts, the fundamental mechanisms of flame propagation in dust suspension have not been sufficiently studied. This is mainly due to experimental difficulties in the generation of a uniform dust suspension, as well as the fact that particle size and size distributions can significantly influence the combustion mechanisms [1,3].

Han et al. [1,4] conducted an experimental study to elucidate the structure of flame propagating through lycopodium dust clouds in a vertical duct. The maximum upward propagating velocity was 0.50 m/s at a dust concentration of 170 g/m^3. Despite the employment of nearly equal sized particles and its good dispersability and flowability, the reaction zone in lycopodium particles cloud showed a double flame structure, consisting of enveloped diffusion flames (spot flame) of individual particles and diffusion flames (independent flame) surrounding some particles.

Kurdyumov and Tarrazo numerically investigated the propagation of premixed laminar flames with different Lewis numbers in open ducts of circular cross-section in a thermal–diffusive model [5]. It was found that when the Lewis number is less than unity, flames velocities in ducts with an isothermal wall may exceed those in ducts with an adiabatic wall of the same diameter. According to this work, this phenomenon is due to the appearance of cellular structures which increase the curvature effect triggered by the boundary conditions at the wall.

Shamim studied the influence of the Lewis number on radiative extinction and flamelet modelling [6]. The results underscored the importance of including the effect of non-unity Lewis numbers and their interaction with chemistry and unsteadiness to improve the predictive capability of flamelet combustion modelling approach and to allow a precise determination of radiation induced extinction limits. It has been notably shown that the steady flame temperature decreased with an increase of the Lewis number and that radiative heat losses were reduced at large Lewis number. Moreover, it has been demonstrated that the Lewis number significantly influences the flame response to unsteadiness. It was also indicated that an increase in the Lewis number in partial premixing improved the incomplete burning of the premixed flame.

* Corresponding author. Tel.: +98 77 240 197; fax: +98 21 77 240 488.
E-mail address: bidabadi@iust.ac.ir (M. Bidabadi).

1290-0729/$ – see front matter © 2009 Elsevier Masson SAS. All rights reserved.
doi:10.1016/j.ijthermalsci.2009.10.002

Nomenclature

x	axial coordinate
t	time
T	temperature
Y_s	mass fraction of the fuel in the solid phase
Y_g	mass fraction of the fuel in the gaseous phase
T_f	flame temperature
T_u	temperature of fresh mixture
t_{vap}	characteristic time of vaporization
t_{chem}	characteristic time of chemical reaction
Da	Damköhler number, t_{vap}/t_{chem}
C	heat capacity of mixture
C_s	specific heat of solid particle
C_p	specific heat of the gaseous phase
D_m	mass diffusion coefficient
Le	Lewis number, $\lambda/\rho C D_m$
E	activation energy of the reaction
R	universal gas constant
Ze	Zeldovich number, $E(T_f - T_u)/RT_f^2$
n_s	local number density of particles (number of particles per unit volume)
r_p	radius of fuel particle
B	frequency factor characterizing rate of gas-phase oxidation of the gaseous fuel
Q	heat reaction
Q_v	latent heat, associated with fuel vaporization
U_f	flame speed
$\widehat{x}$	non-dimensional form of axial coordinate
$\widehat{x}_v$	non-dimensional form of locus where vaporization starts

Greek symbol

ρ	mixture density
ρ_s	density of a fuel particle
λ	thermal conductivity
$\dot{\omega}_{chem}$	rate of chemical reaction
$\dot{\omega}_{vap}$	rate of dust cloud vaporization
θ	non-dimensional form of temperature
θ_v	non-dimensional form of threshold temperature of vaporization
Φ_u	overall equivalence ratio of the initial combustible mixture
ε	expansion parameter, $1/Ze$

In the resumption, Daou et al. [7] derived the analytical expressions for the burning rate of a flame propagating in a prescribed steady parallel flow which scale is much smaller than the laminar flame thickness. The influence of Damköhler, non-unit Lewis numbers and volumetric heat losses were addressed in this research. In particular, it was shown that non-unit Lewis number effects became insignificant in the asymptotic limit.

Proust [8,9] measured the laminar burning velocities and maximum flame temperatures for combustible dust–air mixtures such as starch dust–air mixtures, lycopodium–air mixtures and sulphur flour–air mixtures. Eckhoff clarified the differences and similarities between dust and gases [10]. It has been concluded that there are two basic differences between dusts and gases which are of substantially greater significance in design of safety standards than these similarities. Firstly, the physics of generation and up-keeping of dust clouds and premixed gas/vapour clouds are substantially different. Secondly, contrary to premixed gas flame propagation, the propagation of flames in dust/air mixtures is not limited to the flammable dust concentration range of dynamic clouds.

Babrauskas systematically and scientifically studied the progress of dust explosion [11]. He claimed that the development of knowledge in this area was uneven. He added that the knowledge of ignition of dust clouds was poor according to the literature and that there were very few theories developed in the ignition field despite a century of research.

Fuchihata et al. discussed the flame structure categorized in distributed reaction zone and well-stirred reactor on Borghi's phase diagram [12]. They supposed that the distributed reaction zone was formed when reaction initiates in a low Damköhler number field. The aim of this work was to conduct experiments allowing a better understanding of the flame structure in low Damköhler number fields.

Ross et al. investigated the devolatilisation times of six coals by measuring the centre temperature response for single particles held stationary in a bench scale atmospheric fluidized-bed reactor [13]. A new theoretical model has been used to distinguish between heat transfer and chemical-kinetic control regimes of coal devolatilisation. This model is based on the ratio between the 95% evolution time and the time required for 95% heating of the particle centre versus the modified Damköhler number to Biot number ratio. In this study the modified Damköhler number relates the ratio of the rate of solid reaction via devolatilisation to the rate of heat conduction through the particle which is the driving force for devolatilisation.

Chakraborty et al. presented a thermo-diffusive model to investigate the interaction of non-unity Lewis number and heat loss for laminar premixed flames propagating in a channel [14]. A coordinate system moving with the flame was used to immobilize the flame within the computational domain. Tip opening near the centerline and dead space near the wall were simultaneously observed at Lewis numbers significantly below unity and in presence of high heat losses. This gives rise to a multicellular flame with "funnel-like" shape. At low Lewis numbers for fluid flow opposing the flame motion, an increase in heat losses leads to a transition from inverted "mushroom" to "funnel-shaped" flame.

Chen et al. [15] theoretically, numerically and experimentally studied the trajectories of outwardly propagating spherical flames initiated by an external energy deposition. Emphasis was placed on how to accurately determine the laminar flame speeds experimentally from the time history of the flame fronts for mixtures with different Lewis numbers and ignition energies. It was found that the linear and non-linear extrapolations for flame speed determination were valid only if the flame radius was above a critical value which strongly depends on the Lewis number. At large Lewis numbers, the critical radius is larger than the minimum flame radius used in the experimental measurements, leading to invalid flame speed extrapolation.

In a previous study, Bidabadi and Rahbari analytically investigated the flame propagation through lycopodium dust particles containing uniformly distributed volatile fuel particle [16]. They explored the flame structure mechanism and the effect of temperature difference between gas and particle on the combustion characteristics.

In the present study, the flame propagation mechanism and the structure of combustion zone have been analytically investigated in order to clarify the mechanisms of flame propagation through dust clouds. It is presumed that the fuel particles vaporize first to yield a gaseous fuel, which is oxidized in gas phase and Dufour and Soret effects are neglected. The flame structure is divided into four zones that consists of a preheat zone where the rate of chemical reaction

is small, an extensive particles vaporization zone, an asymptotically thin reaction zone where the convection and the rate of vaporization of the particles are negligible and finally post flame zone. The paper presents an analytical approach within the simple framework of the thermal–diffusive model, which is complemented by a vaporization rate, and then Fick's law and Fourier's law are used to describe diffusion of species and energy transfer. Finally, the effects of different Lewis and Damköhler numbers and the initiation of vaporization on the combustion phenomenon of the organic dust particles are studied in this research.

2. The theoretical model for the combustion of organic dust particles

In the combustion of organic dust particles, the vaporization rate is an effective parameter controlling the combustion phenomenon that elucidates the main difference between organic dust and gas mixture explosion.

Furthermore, the combustion phenomena are not only controlled by the vaporization rate but also by the rate of heat conduction to mass diffusivity. The non-dimensional expression of this ratio is represented by the Lewis number (Le):

$$Le = \frac{\lambda}{\rho C D_m} \tag{1}$$

where λ, ρ, C and D_m are the thermal conductivity of the gaseous mixture, the mixture density, the mixture specific heat and the characteristic mass diffusivity, respectively. In this study, the principal attention is made to investigate the impact of non-unity Lewis number.

In the asymptotic limit, the value of the characteristic Zeldovich number based on the gas-phase oxidation of the gaseous fuel is large. It is defined by:

$$Ze = \frac{E(T_f - T_u)}{RT_f^2} \tag{2}$$

where E, R, T_f and T_u are the activation energy of reaction, the universal gas constant, flame temperature and fresh mixture temperature, respectively.

In the available literatures, the Damköhler number has been explained by various definitions. While the Damköhler number is traditionally defined as the ratio of the characteristic fluid mechanical time to the characteristic chemical time, it was either expressed as the ratio of the mixing time (t_{mix}) to the characteristic reaction time (t_{chem}) by Liñán [17] or defined as the ratio of appropriate characteristic times of conduction to the chemical reaction by Vázquez-Espí and Liñán [18]. In fact, the vaporization Damköhler number (Da) used in this study is defined as the ratio of the vaporization time (t_{vap}) to the characteristic reaction time (t_{chem}) or the ratio of the chemical reaction rate to the vaporization rate.

The main assumption that leads to the aforementioned model of dust combustion within the limit of small organic particles is that Damköhler number is the less than order of unity ($Da < O(1)$), otherwise the combustion process is limited by the vaporization rate. It implies that for the organic dust cloud that contains large particles, combustion process is controlled by vaporization rate, if the vaporization rate (pyrolysis of volatile particles) becomes lower than the reaction rate, i.e., $Da > O(1)$.

It is considered that the flame is propagating through a fresh mixture composed of a homogeneous dispersion of particles, fuel vapor, and air. In order to simplify the governing equations, it is presumed that the particle temperature is equal to the gases temperature. Furthermore, the combustion process is modelled as a one step overall reaction:

$$\nu_F[F] + \nu_{O_2}[O_2] \rightarrow \nu_{\mathrm{Prod}}[P] \tag{3}$$

where the symbols F,O_2 and P denote the fuel, oxygen and product, respectively. Also, the quantities ν_F, ν_{O_2} and ν_{Prod} denote their stoichiometric coefficients. The constant rate of the overall reaction is written in the Arrhenius form.

It is noticing that the fuel particles burn with an envelope diffusion flame surrounding each particle everywhere in the reaction zone for small n_s (local number density of particles). In the analysis developed here, it is assumed that the value of n_s is large enough so that the standoff distance of the envelope flame surrounding each particle is much larger than the characteristic separation distance between the particles.

For the spray combustion of liquid fuel, it is shown that if the overall equivalence ratio of the initial combustible mixture Φ_u is larger than 0.7, therefore the standoff distance of the envelope flame surrounding each particle is larger than the existence distance between particles. This assumption corresponds to the continuity condition in the combustion process. The obtained results for the spray combustion [19] can be used for the combustion of organic dust particle. Therefore it is expected that the developed analytical model validates only for $\Phi_u > 0.7$ (more details can be found in [20]).

The governing equations are written as follow:

1. Particle fuel conservation:

$$\rho \frac{\partial Y_s}{\partial t} + \rho U_f \frac{\partial Y_s}{\partial x} = -\rho \dot{\omega}_{vap} \tag{4}$$

where Y_s, U_f and ρ are the mass fraction of organic dust particle, burning velocity and density of the mixture, respectively. $\dot{\omega}_{vap}$ is the particle vaporization rate which is denoted by:

$$\dot{\omega}_{vap} = \frac{Y_s}{\tau_{vap}} H(T - T_v) \tag{5}$$

where H, τ_{vap}, T, and T_v are the Heaviside function, the constant characteristic time of vaporization, mixture temperature and threshold temperature of vaporization, respectively.

2. Gaseous fuel conservation:

$$\rho \frac{\partial Y_g}{\partial t} + \rho U_f \frac{\partial Y_g}{\partial x} = \rho D_m \frac{\partial^2 Y_g}{\partial x^2} + \rho \dot{\omega}_{vap} - \rho \dot{\omega}_{chem} \tag{6}$$

where Y_g and D_m are the mass fraction of the gaseous fuel gained from the vaporization of organic dust particles and the binary diffusion coefficient of the gaseous limiting component, respectively. $\dot{\omega}_{chem}$ is the rate of the chemical-kinetic expressed by the following relation:

$$\dot{\omega}_{chem} = \rho Y_g B \exp\left(-\frac{E}{RT}\right) \tag{7}$$

3. Energy conservation:

$$\rho C \frac{\partial T}{\partial t} + \rho U_f C \frac{\partial T}{\partial x} = \lambda \frac{\partial^2 T}{\partial x^2} + Q \rho \dot{\omega}_{chem} - Q_v \rho \dot{\omega}_{vap} \tag{8}$$

where Q_v and Q are the latent heat of vaporization and the heat of reaction, respectively. The heat capacity appearing in the above equation is the combined heat capacity of the gas C_p and of the particle C_s, and can be evaluated from the following expression [20]:

$$C = C_p + \frac{4\pi r_p^3 C_s \rho_s n_s}{3\rho} \tag{9}$$

where ρ_s,r_p and n_s are particle density, radius of the particle and the average number of particles per unit volume, respectively.

3. Non-dimensionalization of governing equations

In order to non-dimensionalize the governing equations, some dimensionless parameters for time, axial distance and temperature are defined as follow:

$$\hat{t} = \frac{t}{D_{th}/U_u^2}, \quad \hat{x} = \frac{x}{D_{th}/U_u}, \quad \theta = \frac{T - T_u}{T_f - T_u} \tag{10}$$

with

$$D_{th} = \frac{\lambda}{\rho \cdot C} \tag{11}$$

where $\theta = 0$ denotes that the mixture temperature is equal to the unburned temperature and $\theta = 1$ denotes that the mixture temperature is equal to the flame temperature. The dimensionless burning velocity defined by equation (12) is equal to the ratio between the burning velocity of the fuel/air mixture (U_f) and the calculated burning velocity in which the latent heat of vaporization is neglected (U_u).

$$\hat{U}_f = \frac{U_f}{U_u} \tag{12}$$

Consequently, the dimensionless governing equations are written as follow:

$$\frac{\partial Y_s}{\partial \hat{t}} + \hat{U}_f \frac{\partial Y_s}{\partial \hat{x}} = -\hat{\omega}_{vap} \tag{13}$$

$$\frac{\partial Y_g}{\partial \hat{t}} + \hat{U}_f \frac{\partial Y_g}{\partial \hat{x}} = \frac{1}{Le} \frac{\partial^2 Y_g}{\partial \hat{x}^2} + \hat{\omega}_{vap} - \hat{\omega}_{chem} \tag{14}$$

$$\frac{\partial \theta}{\partial \hat{t}} + \hat{U}_f \frac{\partial \theta}{\partial \hat{x}} = \frac{\partial^2 \theta}{\partial \hat{x}^2} + \hat{\omega}_{chem} \tag{15}$$

where

$$\hat{\omega}_{chem} = \frac{D_{th}}{U_u^2} k Y_g \exp\left[\frac{-Ze(1-\theta)}{1-\alpha(1-\theta)}\right] \tag{16}$$

$$\hat{\omega}_{vap} = \frac{Y_s}{Da} H(\theta - \theta_v) \tag{17}$$

where Damköhler number (Da) is presented by the following expression:

$$Da = \frac{\dot{\omega}_{chem}}{\dot{\omega}_{vap}} = \frac{\tau_{vap}}{\tau_{chem}} \tag{18}$$

Also, α in equation (16) and θ_v in equation (17) are described as:

$$\alpha = \frac{T_f - T_u}{T_f}, \quad \theta_v = \frac{T_v - T_u}{T_f - T_u} \tag{19}$$

As mentioned, the latent heat of vaporization neglected in this research leads to $U_f = U_u$ or $\hat{U}_f = 1$. The constant rate of the overall reaction is written in the Arrhenius form $k = B \exp(-E/RT_f)$ where B represents the frequency factor.

4. Steady state solution

The method used to solve equations (13)–(15) are presented in this section. Within the limit $Ze \to +\infty$, reaction rate is negligible everywhere, except in a small zone located in the vicinity of $\hat{x} = 0$ where $\theta = 1$. Therefore, the flame structure is divided into four regions:

$Z_1 = \{\hat{x} \mid -\infty < \hat{x} < \hat{x}_v\}$ (The preheat zone);
$Z_2 = \{\hat{x} \mid \hat{x}_v \le \hat{x} < 0^-\}$ (The vaporization (devolatilisation) zone);
$Z_3 = \{\hat{x} \mid 0^- \le \hat{x} \le 0^+\}$ (The asymptotically thin reaction zone);
$Z_4 = \{\hat{x} \mid 0^+ < \hat{x} < +\infty\}$ (The post flame zone).

Fig. 1 shows the flame structure for organic dust particles as mentioned above. In the resumption, the analytical method used in this research in order to solve the governing equations associating with boundary conditions and matching equations is presented.

1. The required boundary conditions for zone *I* are as follow:

$$\text{at } \hat{x} \to -\infty \Rightarrow Y_s = 1, \quad Y_g = 0, \quad \theta = 0 \tag{20}$$

2. At the border of zones *I* and *II*, the boundary and matching conditions are:

$$\text{at } \hat{x} = \hat{x}_v \Rightarrow \theta = \theta_v, \quad [Y_s] = [Y_g] = \left[\frac{dY_g}{d\hat{x}}\right] = \left[\frac{d\theta}{d\hat{x}}\right] = 0 \tag{21}$$

where the square brackets denote the jump condition in the quantity enclosed by them. All quantities are continuous, except the first derivative of Y_s.

3. At the interface of zones *II* and *III*, the boundary and matching conditions are:

$$\text{at } \hat{x} = 0^- \Rightarrow Y_g = 0, \quad [\theta] = [Y_g] = \left[\frac{dY_g}{d\hat{x}}\right] = \left[\frac{d\theta}{d\hat{x}}\right] = 0 \tag{22}$$

4. The convection and vaporization terms are considered negligible in the reaction zone in comparison with the reaction and diffusion terms. Integration of reactive diffusive equations (14) and (15) in zone *III* gives the below jump condition:

$$\left[\frac{d\theta}{d\hat{x}} + \frac{1}{Le}\frac{dY_g}{d\hat{x}}\right]_{0^-} = \left[\frac{d\theta}{d\hat{x}} + \frac{1}{Le}\frac{dY_g}{d\hat{x}}\right]_{0^+} \tag{23}$$

Therefore, in order to obtain the flame structure, it is needed to solve the dimensionless governing equations and their required boundary or matching conditions in each zone.

5. The obtained functions in each zone

As mentioned, in zone I and III, the reaction term is neglected contrary to the convection and diffusion ones. Thus, the temperature profile and its boundary conditions are described as:

$$\theta = c_1 + c_2 e^{\hat{x}}, \quad \begin{cases} \hat{x} \to -\infty \Rightarrow \theta = 0 \\ \hat{x} \to 0^- \Rightarrow \theta = 1 \end{cases} \Rightarrow \begin{cases} c_1 = 0 \\ c_2 = 1 \end{cases} \tag{24}$$

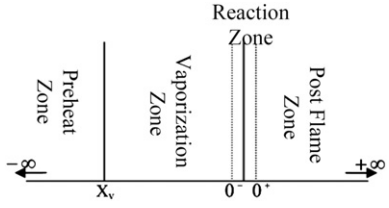

Fig. 1. The flame structure for micro-organic dust particles.

Finally, the dimensionless temperature in zones *I* and *II* is defined as follow:

$$\theta = \exp(\hat{x}) = \exp\left(\frac{\rho U_f C}{\lambda} x\right) \tag{25}$$

Using the boundary condition (21), the point in which the vaporization starts is equal to:

$$\hat{x}_v = \ln \theta_v \tag{26}$$

Other flame structure parameters are determined in each zone as a following consequence.

5.1. Preheat zone $(-\infty < \hat{x} < \hat{x}_v)$

In this zone $(-\infty < \hat{x} < \hat{x}_v)$ where the vaporization rate is zero due to the fact that $\theta < \theta_v$, the mass fraction of particles is equal to unity.

$$Y_s = 1 \tag{27}$$

In order to calculate the mass fraction of gas-phase fuel in this zone, the vaporization and reaction terms are considered negligible in comparison with other terms. Thus:

$$Y_g = c_1 + c_2 \exp(Le\cdot\hat{x}) \tag{28}$$

Using the boundary condition (20) culminates to $c_1 = 0$ and the quantity of c_2 is obtained via the matching condition between zones *I* and *II*. In the resumption the strategy of determining this constant will be revealed.

5.2. Vaporization zone $(\hat{x}_v \le \hat{x} < 0^-)$

The mass fraction of particles in this zone is measured via equations (13) and (17) as follow:

$$Y_s = \exp\left\{-\frac{(\hat{x} - \hat{x}_v)}{Da}\right\} \tag{29}$$

where Y_s, which is at the interface between reaction and vaporization zones, is not zero at $x = 0^-$ and it is equal to $\exp(\hat{x}_v/Da)$ which is very small in the condition of $Da << O(1)$. Substituting equation (26) into equation (29) leads to:

$$Y_s|_{\hat{x}=0^-} = \exp(\hat{x}_v/Da) = \theta_v^{1/Da} \tag{30}$$

In addition, the mass fraction of the gaseous fuel is obtained by substituting equation (29) into equation (17) and by replacing the obtained expression into equation (14) to omit the reaction term.

$$Y_g = b_1 + b_2 \exp(Le\cdot\hat{x}) - \frac{1}{(1 + 1/Le\cdot Da)} \exp\left(-\frac{\hat{x} - \hat{x}_v}{Da}\right) \tag{31}$$

In order to determine the constant coefficient in the above equation, first, by considering $Y_g|_{\hat{x}=0^-} = 0$, the following expression can be written:

$$b_1 + b_2 - \frac{1}{(1 + 1/Le\cdot Da)} \exp\left(\frac{\hat{x}_v}{Da}\right) = 0 \tag{32}$$

Also using the relation (28) and applying the matching conditions between zones *I* and *II* at $\hat{x} = \hat{x}_v$ for Y_g and $dY_g/d\hat{x}$ leads to two new correlations. Therefore there are three unknowns and three correlations and these three unknowns are determined as follow:

$$b_1 = 1 \tag{33}$$

$$b_2 = (1 + 1/Le\cdot Da)^{-1} \exp(\hat{x}_v/Da) - 1 \tag{34}$$

$$c_2 = \exp(-Le\cdot\hat{x}_v)\Big\{1 - (1+1/Le\cdot Da)^{-1} + \exp(Le\cdot\hat{x}_v)\big\langle -1 + (1+1/Le\cdot Da)^{-1} \exp(\hat{x}_v/Da)\big\rangle\Big\} \tag{35}$$

Thus substituting expression (35) into equation (28) yields to the gaseous fuel mass fraction in the zone *I* by:

$$Y_g = \Big\{1 - (1 + 1/Le\cdot Da)^{-1} + \exp(Le\cdot\hat{x}_v)\big\langle -1 + (1 + 1/Le\cdot Da)^{-1} \exp(\hat{x}_v/Da)\big\rangle\Big\} \exp(Le(\hat{x} - \hat{x}_v)) \tag{36}$$

Also replacing equations (33) and (34) into (31) terminates to the gaseous fuel mass fraction in the zone *II* by:

$$Y_g = 1 + \Big\{-1 + (1 + 1/Le\cdot Da)^{-1} \exp(\hat{x}_v/Da)\Big\} \times \exp(Le\cdot\hat{x}) - (1 + 1/Le\cdot Da)^{-1} \exp\left(-\frac{\hat{x} - \hat{x}_v}{Da}\right) \tag{37}$$

The location in which the quantity of Y_g is in its peak can be achieved by derivation from equation (37) as follow:

$$\hat{x}_{\max} = (1 + Le\cdot Da)^{-1}\big\langle \hat{x}_v - Da\cdot \ln\{1 + Le\cdot Da[1 - \exp(\hat{x}_v/Da)]\}\big\rangle \tag{38}$$

where in the above equation $\hat{x}_{\max}$ is larger than $\hat{x}_v$.

5.3. Post flame zone $(0^+ < \hat{x} < +\infty)$

Before analyzing the reaction zone, the post flame zone is primarily investigated due to the fact that its study is more simplified than the reaction zone one. Furthermore, the matching conditions needed for the reaction zone can be attained by explaining this zone. Therefore:

$$\theta = 1, \quad Y_s \cong cte, \quad Y_g = 0 \tag{39}$$

The available mass fraction of solid particles in post flame zone is approximately equal to the quantity of Y_s at the end of the vaporization zone (i.e., $\hat{x} = 0^-$) due to the matching condition.

5.4. Reaction zone $(0^- \le \hat{x} \le 0^+)$

In this region, the convective and vaporization terms in the conservation equations are presumed to be small in comparison with the diffusive and reactive terms.

In order to analyze the structure of this zone the following expressions

$$\hat{x} = \varepsilon\xi, \quad Y_g = \varepsilon(s + y), \quad \theta = 1 - \varepsilon r \tag{40}$$

are introduced, where $s = Y_g|_{\hat{x}=0^-}/\varepsilon$ and $\varepsilon = 1/Ze$ is the expansion parameter, which is presumed to be small. The quantities s and r are assumed to be of the order of unity. Substituting expansions (40) into equations (14) and (15) yields to the following expressions, respectively:

$$\frac{1}{Le}\frac{d^2y}{d\xi^2} = \frac{D_{th}k\varepsilon^2}{U_f^2}(s + y)\exp(-r) \tag{41}$$

$$\frac{d^2r}{d\xi^2} = \frac{D_{th}k\varepsilon^2}{U_f^2}(s+y)\exp(-r) \tag{42}$$

Combining the equations (41) and (42) results to the following expression:

$$\frac{d^2(r - Le^{-1}y)}{d\xi^2} = 0 \tag{43}$$

Boundary condition for above equation is determined via the matching condition with the solution in the post flame zone for $\xi \to +\infty$ as follow:

$$\frac{dr}{d\xi} = \frac{dy}{d\xi} = 0 \quad \xi \to +\infty \tag{44}$$

Integrating twice from equation (43) and utilizing expression (44) lead to $r = Le^{-1}y$. Matching with the vaporization zone results to:

$$\frac{dr}{d\xi} = -1 \quad \xi \to -\infty \tag{45}$$

The equation (42) can be integrated once and using the boundary conditions (44) and (45) yields the below result:

$$\frac{2D_{th}k\varepsilon^2}{U_f^2}(s+Le) = 1 \tag{46}$$

The constant s is attained by:

$$\begin{aligned} s &= \frac{Y_g|_{\widehat{x}=0^-}}{\varepsilon} = \frac{Y_g|_{\widehat{x}=-\varepsilon}}{\varepsilon} \\ &= \frac{1}{\varepsilon}\Bigg\langle 1 + \Big\{-1 + (1+1/Le\cdot Da)^{-1}\exp(\widehat{x}_v/Da)\Big\} \\ &\quad \times \exp(-Le\cdot\varepsilon) - (1+1/Le\cdot Da)^{-1}\exp\left(\frac{\varepsilon+\widehat{x}_v}{Da}\right)\Bigg\rangle \end{aligned} \tag{47}$$

Using equation (46) and substituting s, k, ε and D_{th} by the correlation obtained previously, the expression of the burning velocity of the micro-organic dust particles becomes:

$$\begin{aligned} U_f^2 &= \frac{2\lambda B}{\rho C Ze^2}\times\Bigg[Ze\Bigg\langle 1 + \Big\{-1 + (1+1/Le\cdot Da)^{-1} \\ &\quad \times \exp(\widehat{x}_v/Da)\Big\}\exp(-Le\cdot Ze^{-1}) - (1+1/Le\cdot Da)^{-1} \\ &\quad \times \exp\left(\frac{Ze^{-1}+\widehat{x}_v}{Da}\right)\Bigg\rangle + Le\Bigg]\times\exp\left(\frac{-E}{RT_f}\right) \end{aligned} \tag{48}$$

Using the matching condition (23), noting that each of the expression in the right side of the above equation is too small and can be neglected and replacing the left side of the above equation by correlations (25) and (37) leads to the useful expression for the Da number as a function of Ze and θ_v described as $Da \cong \log^{\theta_v}_{2/Ze}$.

6. Results and discussion

In order to demonstrate the accuracy of the model proposed here, simulation results obtained with this model are compared with experimental and theoretical data.

As seen in Fig. 2, the evolution of the burning velocity as a function of the mass particle concentration is in reasonable agreement with the experimental trend issued from the results published by Proust [9]. This implies that the burning velocity increases when the mass particle concentration grows. The obtained result from this model is closer to the direct method data than the tube method data. There are two main reasons which can explain the differences observed between the results obtained with this model and the results issued from the correlation of Proust [9]: first thermal radiation induced from flame interface into unburned zone, secondly heat recirculation from the surrounding walls of the reaction and burned zones to preheat and vaporization zones. Indeed, it is needed to note that these effects are not applied into the governing equations in this research. These factors improve the vaporization of the organic dust particles which results in the increase of the burning velocity.

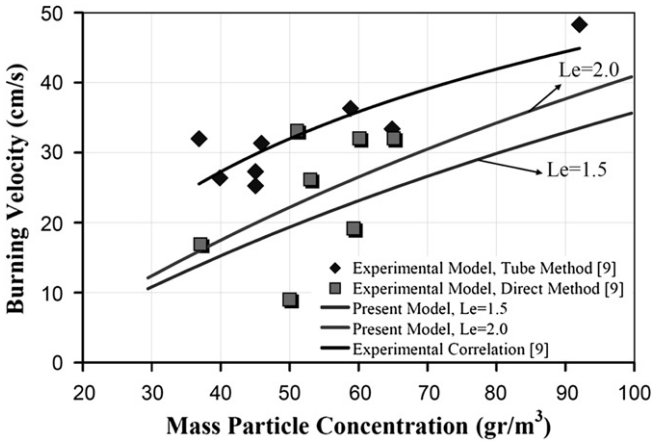

Fig. 2. The variation of burning velocity as a function of mass particle concentration for both present model and experimental published data.

The tendency obtained for the variation of the burning velocity as a function of the equivalence ratio (defined as the quantity of fuel available in the particles) is similar to that of the Seshadri [20], as shown in Fig. 3. This figure illustrates that for a given radius, the burning velocity increases when the equivalence ratio rises. On the other hand, the burning velocity increases when the radius of the particles passes from 100 to 10 μm. This is probably due to the fact that the contact surface between the oxidizer and the particles is much more important when the radius is small.

The main discrepancy between the present model and the previous analytical results [16,20] is that in this model the flame structure is divided into four zones including the emphasis on the

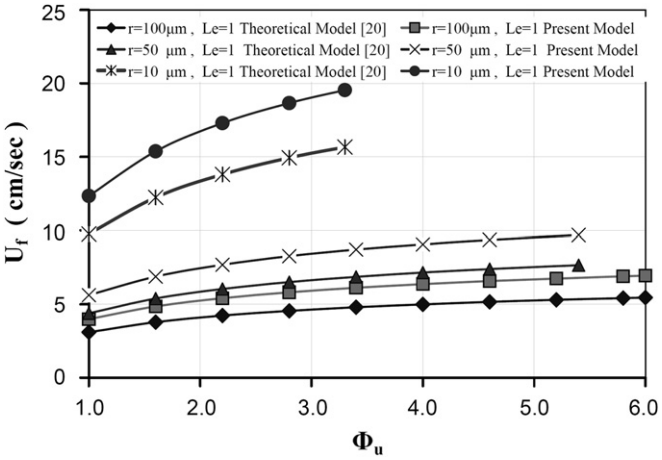

Fig. 3. The variation of burning velocity as a function of equivalence ratio for different radius of the particle for both present model and theoretical published data.

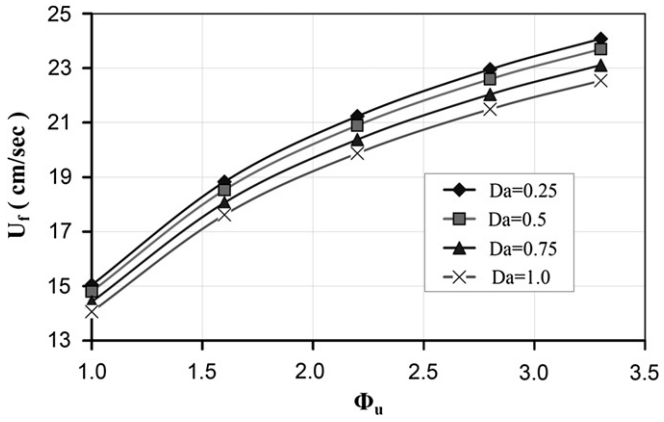

Fig. 4. The variation of burning velocity as a function of equivalence ratio for different Damköhler numbers at $r_p = 10\,\mu m$, $Le = 1.25$.

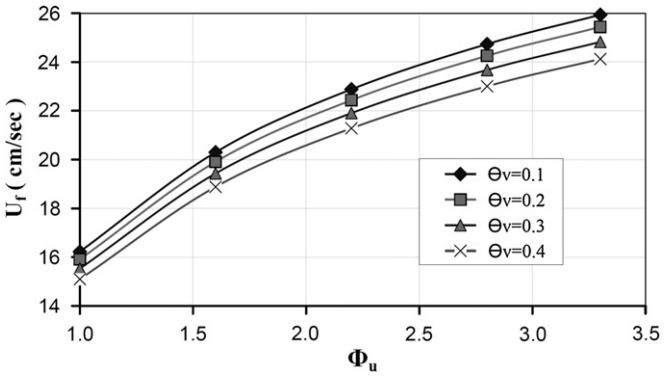

Fig. 6. The variation of burning velocity as a function of equivalence ratio for different dimensionless temperature in the onset of vaporization at $r_p = 10\,\mu m$, $Le = 1.5$, $Da = 0.75$.

onset of vaporization while in the previous models the flame structure is composed of three zones and the role of the initiation of vaporization was ignored. Furthermore, the new expression for the vaporization rate of volatile fuel particles has been used in this research in comparison with the available theoretical models [16,20].

As observed in Fig. 4, the trend of the diagram goes down when the quantity of Da number is shooting up from 0.25 to 1.0 at $r_p = 10\,\mu m$ and $Le = 1.25$. Based on the Da number definition, rising this number results to increase in the rate of reaction to vaporization rate, thus, the gaseous fuel can not supply the high amount of reaction rate, and consequently the burning velocity decreases.

The burning velocity is strongly affected by the variation of the Lewis number, as shown in Fig. 5. It demonstrates that the burning velocity remarkably increases when the Lewis number grows from 0.75 to 1.5 at $r_p = 10\,\mu m$ and $Da = 0.25$. In fact, the increase in Lewis number (the ratio of thermal diffusivity to mass diffusivity) associates with the noticeable rise in the thermal diffusivity which improves both the vaporization process of volatile fuel particles and the burning velocity of two-phase mixture.

In the resumption, the effect of the dimensionless temperature at the onset of vaporization on the burning velocity is illustrated in Fig. 6 at $r_p = 10\,\mu m$, $Le = 1.5$ and $Da = 0.75$. As seen in this figure, increasing the θ_v from 0.1 to 0.4 implies that for initializing the vaporization process, the higher temperature is needed, therefore, the onset of vaporization becomes closer to the reaction zone and consequently there is not enough time for the vaporization of the volatile fuel particles. Indeed, all of these events cause a reduction of the burning velocity.

As seen in Fig. 7, the mass fraction of dust particles increases along the non-dimensional distance of the flame structure when the Da number elevates from 0.25 to 1.0 at $\theta_v = 0.25$. As mentioned, higher Da number signifies that the vaporization rate declines. Fig. 8 illustrates the variation of organic dust mass fraction with non-dimensional distance for the various numbers of θ_v at $Da = 0.25$. As mentioned above, when θ_v augments the higher

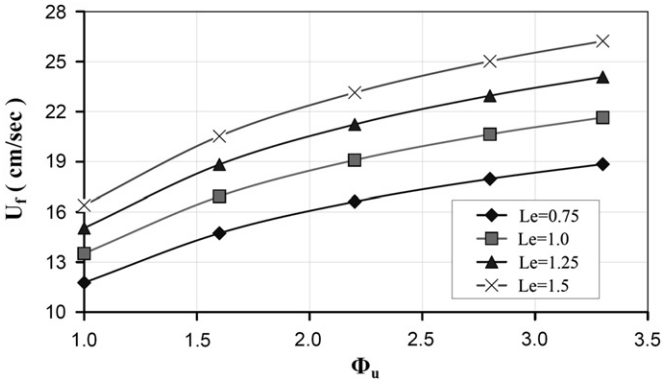

Fig. 5. The variation of burning velocity as a function of equivalence ratio for different Lewis numbers at $r_p = 10\,\mu m$, $Da = 0.25$.

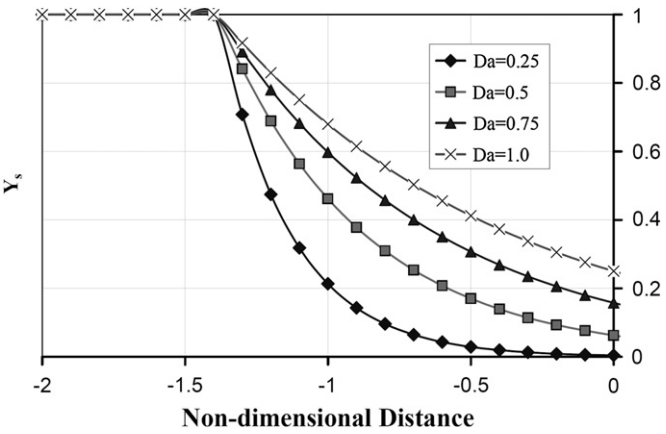

Fig. 7. The variation of organic dust mass fraction as a function of non-dimensional distance for different Damköhler numbers at $\theta_v = 0.25$.

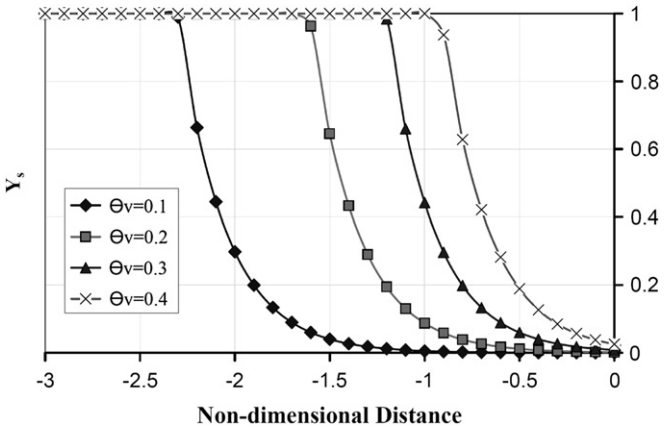

Fig. 8. The variation of organic dust mass fraction as a function of non-dimensional distance for different θ_v at $Da = 0.25$.

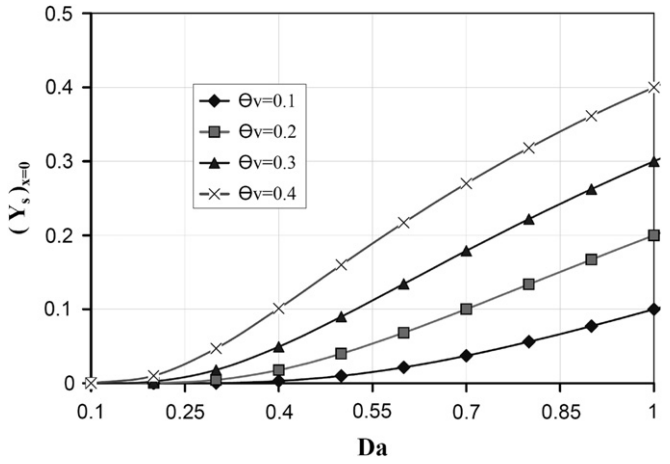

Fig. 9. The variation of organic dust mass fraction at $x = 0$ as a function of Damköhler number for different θ_v.

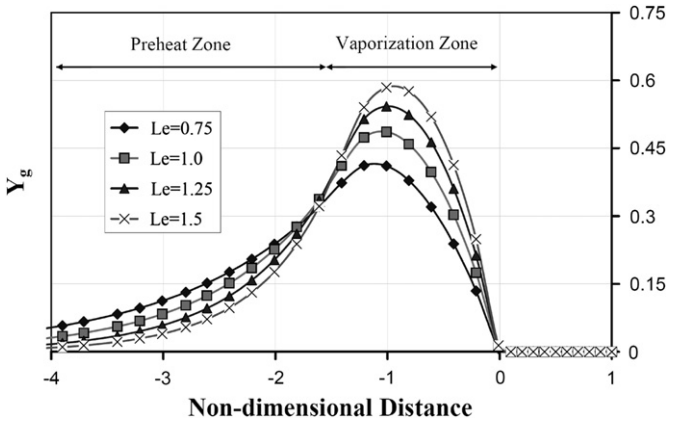

Fig. 11. The variation of gaseous fuel mass fraction gained from the vaporization of the lycopodium particles as a function of non-dimensional distance for different Lewis numbers at $\theta_v = 0.25$, $Da = 0.5$.

temperature is needed for vaporization of volatile fuel particles. Thus, the mass fraction diagram shifts to the right side near the reaction zone.

One of the important parameters which should be determined in the combustion of organic dust is the quantity of organic dust mass fraction as a function of different *Da* numbers at the initiation of combustion, as shown in Fig. 9. As perceived, at the lower *Da* numbers (lower than 0.15), the amount of mass fraction is not influenced by the variation of θ_v, while at the higher *Da* numbers, the trend is upside down. This implies that elevating the θ_v has the highlighted impact on the mass fraction of solid particles at initiation of combustion and causes to shoot up this quantity.

Fig. 10 shows the variation of gaseous fuel mass fraction as a function of non-dimensional distance. As seen, the quantity of Y_g declines when the *Da* number grows from 0.25 to 1 because the rise in the *Da* numbers corresponds with the slower rate of vaporization.

Fig. 11 presents the effect of various Lewis numbers on the behaviour of gaseous fuel mass fraction. As seen, the quantity of gaseous fuel mass fraction at the vaporization zone grows when Lewis number elevates from 0.75 to 1.5 which is probably due to the fact that higher Lewis numbers provide better vaporization process, but the vaporization of volatile fuel particle has not been initiated in the preheat zone and the existent amount of Y_g is caused by the mass diffusion from the vaporization zone interface $(\hat{x}_v)$ into this region. In fact, the increase in the *Le* number associates with the reduction in the value of mass diffusion implies that the Y_g decreases in the preheat zone when the *Le* number grows, as seen in this figure.

In order to better observe the significant impact of θ_v on the combustion of organic dust particles, the variation of gaseous fuel

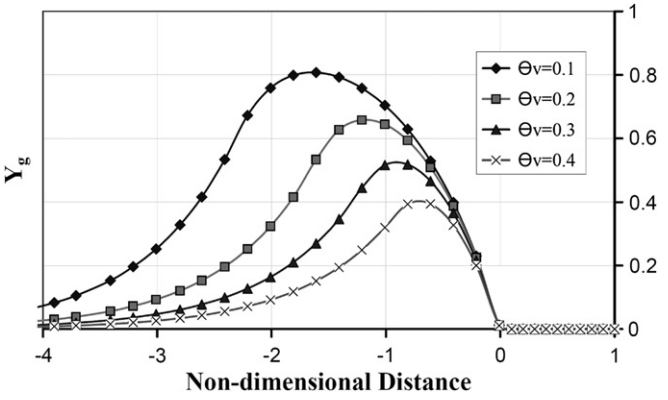

Fig. 12. The variation of gaseous fuel mass fraction gained from the vaporization of the lycopodium particles as a function of non-dimensional distance for different θ_v at $Le = 1.25$, $Da = 0.4$.

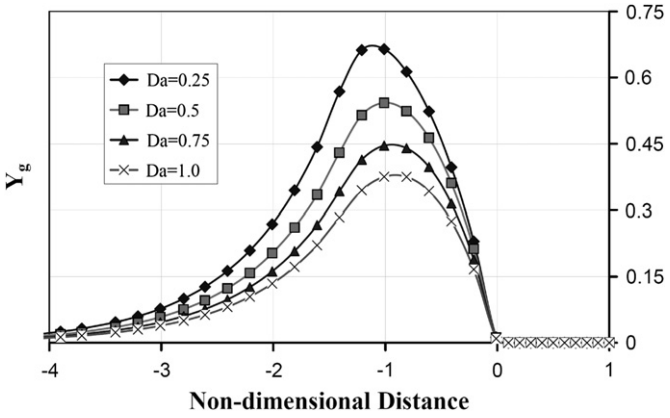

Fig. 10. The variation of gaseous fuel mass fraction gained from the vaporization of the lycopodium particles as a function of non-dimensional distance for different Damköhler numbers at $\theta_v = 0.25$, $Le = 1.25$.

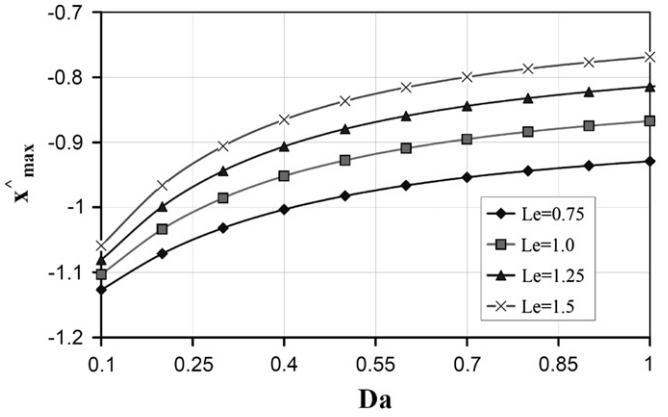

Fig. 13. The variation of the location in which the quantity of gaseous fuel mass fraction is in its peak as a function of Damköhler numbers for different Lewis numbers at $\theta_v = 0.3$.

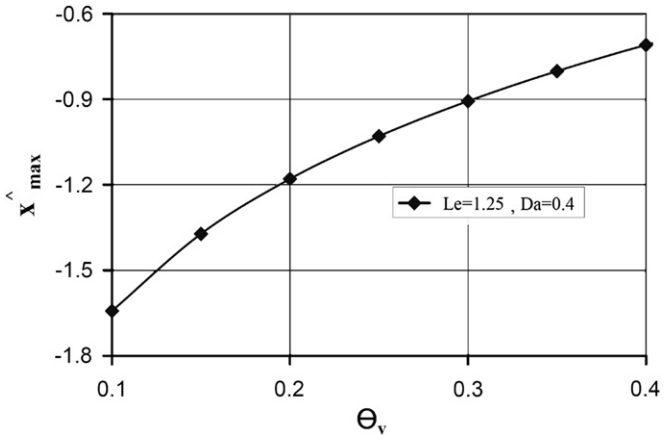

Fig. 14. The variation of the location in which the quantity of gaseous fuel mass fraction is in its peak as a function of θ_v at $Le = 1.25$, $Da = 0.4$.

mass fraction with non-dimensional distance for different θ_v at $Le = 1.25$ and $Da = 0.4$ is plotted in Fig. 12. As presented in this figure, the increase in θ_v leads to decrease in the amount of Y_g and the onset of vaporization and the maximum of diagram also shift to the right side near the reaction zone.

Fig. 13 illustrates the variation of the location in which the quantity of gaseous fuel mass fraction is in its peak as a function of Damköhler numbers for different Lewis numbers. As seen, $\hat{x}_{max}$ approaches to the reaction zone due to the increase in the *Da* number from 0.1 to 1.0 and *Le* number from 0.75 to 1.5 which can be explained by the definition of *Da* and *Le* numbers.

Finally, $\hat{x}_{max}$ is plotted as a function of θ_v at $Le = 1.25$ and $Da = 0.4$ in Fig. 14. It demonstrates that the quantity of $\hat{x}_{max}$ exponentially increases with θ_v(i.e., approaches to the reaction zone).

7. Conclusions

In this research, the flame propagation through micro-organic dust particles is analytically analyzed and it is presumed that the particles vaporize first to yield the known chemical structure before entering the reaction zone. In order to simulate the flame structure, it is assumed that the structure of flame consists of four zones as preheat, vaporization, reaction and post flame zone.

Then the governing equations are non-dimensionalized and these equations associating with their boundary and matching conditions are solved simultaneously. Consequently the burning velocity profile obtained from this model is compared with the experimental published data [9] and the comparison demonstrates that this model accurately predicts the behaviour of burning velocity. In addition, the burning velocity profile from this model is compared with the model presented in [20], and it is observed that the vaporization zone added in this research has the considerable effect on the burning velocity.

Damköhler and Lewis numbers are the determining factors on the combustion of dust particles and it is seen that increase in the *Da* number causes a reduction in the burning velocity. Moreover, the higher burning velocity gains at lower radius of the particle. In addition, when the Lewis number elevates, the amount of burning velocity augments due to the increase in the thermal diffusivity.

Furthermore, the increase in the θ_v associates with the decrease in the burning velocity which physically implies that at higherθ_v, the higher temperature is needed for starting the vaporization process. Also when θ_v goes up, mass fraction of the organic dust particles moves towards the reaction zone. It is illustrated that the mass fraction of the organic dust particles is more influenced by the *Da* numbers.

The variation of gaseous fuel mass fraction with different *Da* number signifies that the amount of Y_g decreases when the *Da* number increases. Furthermore, gaseous fuel mass fraction at preheat and vaporization zones goes down and up respectively when the *Le* number increases.

The increase in θ_v culminates to decrease in the amount of the gaseous fuel mass fraction and in addition the onset of the vaporization and maximum of the diagram move towards the reaction zone. The role of increasing in θ_v, *Le* and *Da* numbers implies that $\hat{x}_{max}$ approaches towards the reaction zone.

References

[1] O.-S. Han, M. Yashima, T. Matsuda, H. Matsui, A. Miyake, T. Ogawa, Behaviour of flame propagating through lycopodium dust clouds in a vertical duct. J. Loss Prev. Process Ind. 13 (6) (2000) 449–457.
[2] K.L. Cashdollar, Overview of dust explosibility characteristics. J. Loss Prev. Process Ind. 13 (2000) 183–199.
[3] R.K. Eckhoff, Dust Explosion in the Process Industries, second ed. Butterworth Heinemann, Oxford, 1997.
[4] O.-S. Han, M. Yashima, T. Matsuda, H. Matsui, A. Miyake, T. Ogawa, A study of flame propagation mechanisms in lycopodium dust clouds based on dust particles' behaviour. J. Loss Prev. Process Ind. 14 (2001) 153–160.
[5] V.N. Kurdyumov, E. Fernández-Tarrazo, Lewis number effect on the propagation of premixed laminar flames in narrow open ducts. Combust. Flame 128 (2002) 382–394.
[6] T. Shamim, The effect of Lewis number on radiative extinction and flamelet modeling. Int. J. Heat Mass Tran. 45 (2002) 1249–1259.
[7] J. Daou, J. Dold, M. Matalon, The thick flame asymptotic limit and Damköhler's hypothesis. Combust. Theory Model. 6 (2002) 141–153.
[8] C. Proust, A few fundamental aspects about ignition and flame propagation in dust clouds. J. Loss Prev. Process Ind. 19 (2006) 104–120.
[9] C. Proust, Flame propagation and combustion in some dust–air mixtures. J. Loss Prev. Process Ind. 19 (2006) 89–100.
[10] R.K. Eckhoff, Differences and similarities of gas and dust explosions: a critical evaluation of the European 'ATEX' directives in relation to dusts. J. Loss Prev. Process Ind. 19 (2006) 553–560.
[11] V. Babrauskas, Ignition: a century of research and an assessment of our current status. J. Fire Prot. Eng. 17 (2007) 165.
[12] M. Fuchihata, M. Katsuki, Y. Mizutani, T. Ida, Observation of the flame structures emerging at low Damköhler number fields. Proc. Combust. Inst. 31 (2007) 1353–1359.
[13] D.P. Ross, C.A. Heidenreich, D.K. Zhang, Devolatilisation times of coal particles in a fluidised-bed. Fuel 79 (2000) 873–883.
[14] S. Chakraborty, A. Mukhopadhyay, S. Sen, Interaction of Lewis number and heat loss effects for a laminar premixed flame propagating in a channel. Int. J. Thermal Sci. 47 (2008) 84–92.
[15] Z. Chen, M.P. Burke, Y. Ju, Effects of Lewis number and ignition energy on the determination of laminar flame speed using propagating spherical flames. Proc. Combust. Inst. 22 (2009) 1253–1260.
[16] M. Bidabadi, A. Rahbari, Modeling combustion of lycopodium particles by considering the temperature difference between the gas and the particles. Combust. Expl. Shock Waves 45 (2009) 49–57.
[17] A. Liñán, Lewis Number Effects on the Structure and Extinction of Diffusion Flames Due to Strain, , In: Lecture Notes in Physics, vol. 136. Springer, Berlin/Heidelberg, 1981, ISBN 978-3-540-10289-2, pp. 333–339.
[18] C. Vázquez-Espí, A. Liñán, Thermal–diffusive ignition and flame initiation by a local energy source. Combust. Theory Model. 6 (2002) 297–315.
[19] F.A. Williams, Combustion Theory, second ed. Addi-son-Wesley, Redwood City, CA, 1985.
[20] K. Seshadri, A.L. Berlad, V. Tangirala, The structure of premixed particle-cloud flames. Combust. Flame 89 (1992) 333–342.